INSTITUTE OF PHYSICS PUBLISHING JOURNAL OF OPTICS B: QUANTUM AND SEMICLASSICAL OPTICS
J. Opt. B: Quantum Semiclass. Opt. **6** (2004) 367–372 PII: S1464-4266(04)76529-5

Quantum fluctuations around bistable solitons in the cubic–quintic nonlinear Schrödinger equation

Ray-Kuang Lee[1], **Yinchieh Lai**[1] **and Boris A Malomed**[2]

[1] Institute of Electro-Optical Engineering, National Chiao-Tung University, Hsinchu, Taiwan 300, Republic of China
[2] Department of Interdisciplinary Studies, School of Electrical Engineering, Faculty of Engineering, Tel Aviv University, Tel Aviv 69978, Israel

E-mail: yclai@mail.nctu.edu.tw and malomed@eng.tau.ac.il

Received 23 February 2004, accepted for publication 26 May 2004
Published 17 June 2004
Online at stacks.iop.org/JOptB/6/367
doi:10.1088/1464-4266/6/9/001

Abstract
Small quantum fluctuations in solitons described by the cubic–quintic nonlinear Schrödinger equation (CQNLSE) are studied within the linear approximation. The cases of both self-defocusing and self-focusing quintic terms are considered (in the latter case, the solitons may be effectively stable, despite the possibility of collapse). The numerically implemented back-propagation method is used to calculate the optimal squeezing ratio for the quantum fluctuations versus the propagation distance. In the case of self-defocusing quintic nonlinearity, opposite signs in front of the cubic and quintic terms make the fluctuations around bistable pairs of solitons (which have different energies for the same width) totally different. The fluctuations of nonstationary Gaussian pulses in the CQNLSE model are also studied.

Keywords: quantum fluctuations, quantum noise, optical solitons, nonlinear guided waves, optical bistability

(Some figures in this article are in colour only in the electronic version)

1. Introduction

Quantum-noise squeezing is one of aspects of quantum mechanics that can exhibit completely different characteristics when compared to the predictions of classical mechanics. Many proposed applications in quantum measurement and quantum information have utilized squeezed states to achieve their goals. Solitons in optical fibres have been known to serve as a platform for demonstrating macroscopic quantum optical fields that exhibit profound kinds of quantum properties including quadrature-field squeezing. Since the nonlinear Schrödinger equation (NLSE) is typically used to model solitons in optical fibres with third-order nonlinearity (Kerr effect), most of the previous studies of the quantum properties of optical solitons were based on the quantum NLSE model [1–5]. Due to the cubic nonlinearity of the fibre, the temporal solitons get squeezed quantum-mechanically during the propagation, i.e., the variance of the perturbed quadrature field operator of the soliton (its exact definition is given below) is smaller than that of the vacuum state. The physics behind this phenomenon is that the nonlinear self-phase-modulation effect induces a correlation between the quantum photon number perturbation (in-phase quadrature component) and the quantum phase perturbation (out-of-phase quadrature component). By choosing a suitable detection phase angle, one can detect a linear combination of the two quadrature components in such a way that the net noise is reduced due to the correlation. This is the simple physical picture that can explain how quadrature squeezing occurs through the Kerr nonlinearity. With the advance of stable pulse laser sources and high-quantum-efficiency detectors at optical communication wavelengths, many experiments have actually demonstrated soliton squeezing [6–8].

It is well known that cubic-NLSE solitons are unstable in higher dimensions (two and three) due to the occurrence of collapse in these cases. However, generalized NLSEs with a

saturable nonlinear response can support multi-stable solitons in multi-dimensional cases [9–15], which opens the way to the creation of stable optical spatiotemporal solitons ('light buttes') in the two- and three-dimensional cases [16, 17].

The general form of the generalized NLSE with saturable nonlinearity is (in the temporal domain)

$$iU_z + U_{tt} + \mathcal{F}(|U|^2)U = 0, \tag{1}$$

where $U(z,t)$ is the local amplitude of the electromagnetic wave, z and t are, as usual, the propagation distance and reduced time, and the function $\mathcal{F}(|U|^2)$ describes the saturable nonlinear response of the medium. Its simplest form, $\mathcal{F}(|U|^2) = |U|^2 - b|U|^4$, corresponds to the cubic–quintic (CQ) nonlinearity, where b is the ratio of the cubic and quintic nonlinear susceptibilities.

In qualitative terms, one may expect that the more peak power the soliton has, the more quadrature squeezing it will experience owing to the higher nonlinear effect. A general question is how the quantum fluctuations around the soliton are affected by the high-order nonlinearity. To the best of our knowledge, the quantum treatment of solitons in the NLSE with CQ nonlinearity (to be abbreviated as CQNLSE) has not yet been worked out. The objective of this work is to do this, in the simplest (1 + 1)-dimensional case, by means of the known *back-propagation method* [18]. We will investigate the quantum fluctuations of the soliton quadrature field components as a function of the distance travelled by the pulse. The measurement scheme that can enable the observation of the predicted effects is *homodyne detection*, which measures the inner product between the given pulse and a local-oscillator gauge pulse, according to the projection interpretation of homodyne detection [19].

The CQNLSE applies, in particular, to light propagation in chalcogenide glasses [20] and some organic materials [21], provided that the nonlinear absorption may be neglected. Therefore, our theoretical results may be tested in these media. Actually, the CQNLSE is the simplest model that allows for the existence of bistable solitons, hence the results reported below may also apply to a broader class of optical media than those which are directly modelled by the combination of the cubic and quintic terms (although the solitons' stability may not be the same in models with different forms of nonlinearity [22]).

The results obtained in the present work can be summarized as follows. First of all, we find that the optimal squeezing ratio of the soliton quadrature field improves when both the cubic and quintic terms are of the same (focusing) sign. On the other hand, the optimal quadrature squeezing ratio degrades when the cubic term is focusing and the quintic one is defocusing. Secondly, the quantum fluctuations around two solitons with equal widths, belonging to a bistable pair, are found to be totally different due to the effect of the quintic nonlinearity. The quantum fluctuations around nonstationary bistable Gaussian pulses are also studied, for comparison with the stationary solitons.

The paper is organized as follows. In section 2, we derive the quantum CQNLSE model and the corresponding linearized and adjoint equations for the quantum fluctuations. The effects of the quintic nonlinearity on the quantum fluctuations, and the difference between the equal-width solitons belonging to a bistable pair, are highlighted in section 3. Section 4 deals with the fluctuations around the nonstationary Gaussian pulses, and compares the results with those for the soliton cases. The paper is concluded by section 5.

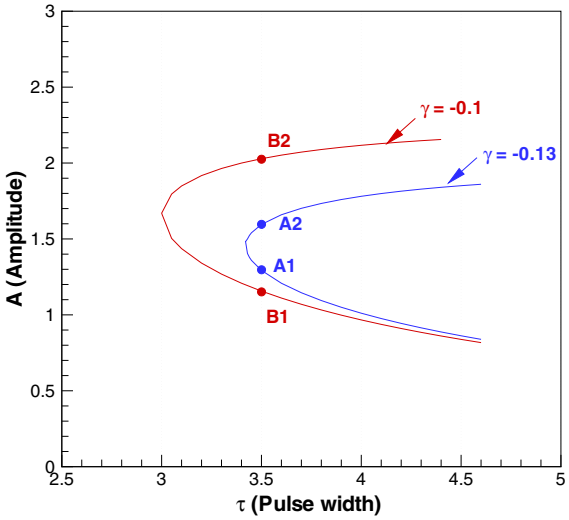

Figure 1. The amplitude–pulsewidth relation for bistable solitons as per equation (4). Two pairs of bistable solitons with equal pulsewidth, $A_{1,2}$ and $B_{1,2}$, are selected as examples for detailed investigation.

2. The quantum cubic–quintic nonlinear Schrödinger equation

The cubic–quintic version of the NLSE (1) is

$$iU_z + U_{tt} + 2\chi|U|^2U + 3\gamma|U|^4U = 0, \tag{2}$$

where the cubic coefficient is normalized to be $\chi = \pm 1$. Solutions for bistable solitons are available in an analytical form [13, 15],

$$U(z,t) = \sqrt{\frac{2\beta}{\sqrt{1+4\gamma\beta}\cosh(2\sqrt{\beta}t) + \chi}}\, e^{i\beta z} \tag{3}$$

where β is the propagation constant (an intrinsic parameter of the soliton family), subject to conditions $\beta > 0$ and $1 + 4\gamma\beta > 0$. The peak power of the solution (3), $A^2 = 2\beta/\left(\sqrt{1+4\gamma\beta} + \chi\right)$, is related to the soliton's full-width at half-maximum pulse width, τ, by the following relation:

$$\cosh\left(\frac{1}{2}\tau\sqrt{\chi A^2 + \gamma A^4}\right) = \frac{3\chi + 4\gamma A^2}{\chi + 2\gamma A^2}. \tag{4}$$

The amplitude–pulsewidth relation for the solitons, given by equation (4), is displayed in figure 1 for $\chi = +1$ and $\gamma < 0$ (the usual case of the self-focusing cubic and self-defocusing quintic nonlinearities). As is seen, the pulsewidth of the soliton cannot be smaller than a minimum (critical) value, which is $\approx$3.0 for $\gamma = -0.1$ and $\approx$3.42 for $\gamma = -0.13$. Two pairs of bistable solitons with identical pulsewidths, marked as A (which is close to the turning point) and B (taken farther from the turning point), are chosen as illustrative examples. In particular, the pulsewidth of the bistable solitons belonging to the pair B is 3.5, and their amplitudes are 1.147 and 2.033,

respectively. Solitons belonging to both branches of the curve in figure 1 are stable (as classical solutions).

In quantum theory, the classical CQNLSE (2) is replaced by its quantum counterpart, with $U(z,t)$ directly replaced by the operator field variable $\hat{U}(z,t)$,

$$\hat{U}_z = \mathrm{i}\hat{U}_{tt} + 2\mathrm{i}\chi\hat{U}^\dagger\hat{U}\hat{U} + 3\mathrm{i}\gamma\hat{U}^\dagger\hat{U}^\dagger\hat{U}\hat{U}\hat{U}. \tag{5}$$

The quantized field operators must satisfy the equal-coordinate Bosonic commutation relations,

$$\begin{aligned}\left[\hat{U}(z,t_1),\hat{U}^\dagger(z,t_2)\right] &= \delta(t_1-t_2),\\ \left[\hat{U}(z,t_1),\hat{U}(z,t_2)\right] &= \left[\hat{U}^\dagger(z,t_1),\hat{U}^\dagger(z,t_2)\right] = 0.\end{aligned} \tag{6}$$

Equation (5), which provides for the Heisenberg-picture description, can be derived from the Hamiltonian

$$\hat{H} = -\int_{-\infty}^{+\infty}\mathrm{d}t\left(\hat{U}^\dagger\frac{\partial^2}{\partial t^2}\hat{U} + \chi\hat{U}^\dagger\hat{U}^\dagger\hat{U}\hat{U} + \gamma\hat{U}^\dagger\hat{U}^\dagger\hat{U}^\dagger\hat{U}\hat{U}\hat{U}\right),$$

so that equation (5) is tantamount to $\mathrm{i}\hat{U}_z = [\hat{U},\hat{H}]$ (the replacement of the ordinary equal-time correlation relations for the quantum fields by the equal-coordinate ones can be justified, in the present physical context, within the framework of the canonical approach, as shown in [23]).

Next, we substitute $\hat{U} = U_0 + \hat{u}$ into equation (5) to linearize the equation around the classical solution U_0 for the soliton containing a very large number of photons, which yields

$$\begin{aligned}\hat{u}_z &= \mathrm{i}\hat{u}_{tt} + 4\mathrm{i}\chi|U_0|^2\hat{u} + 9\mathrm{i}\gamma|U_0|^4\hat{u}\\ &\quad + 2\mathrm{i}\chi U_0^2\hat{u}^\dagger + 6\mathrm{i}\gamma U_0^3U_0^*\hat{u}^\dagger \equiv \hat{\mathcal{P}}\hat{u},\end{aligned} \tag{7}$$

where $\hat{\mathcal{P}}$ is an effective evolution operator. The operator perturbation field $\hat{u}$ obeys the same equal-coordinate Bosonic commutation relations (6) as the unperturbed field operator $\hat{U}$.

To describe the quantum fluctuations, we need to find the corresponding linear adjoint field which satisfies the condition

$$\langle u^{\mathrm{A}}|\hat{\mathcal{P}}\hat{u}\rangle = \langle\hat{\mathcal{P}}^{\mathrm{A}}u^{\mathrm{A}}|\hat{u}\rangle, \tag{8}$$

where $\hat{\mathcal{P}}^{\mathrm{A}}$ is the adjoint operator of $\hat{\mathcal{P}}$ and the inner product is defined by

$$\langle f|\hat{g}\rangle = \tfrac{1}{2}\int_{-\infty}^{+\infty}\left(f^*\hat{g} + f\hat{g}^\dagger\right)\mathrm{d}t. \tag{9}$$

This definition of the inner product conforms to the principle that any physical observable can be expressed as the inner product between a characteristic measurement function and the quantum-field operator of the observable [18]. The adjoint field which implements the condition in equation (8) obeys the following linear operator equation:

$$\begin{aligned}u_z^{\mathrm{A}} &= \mathrm{i}u_{tt}^{\mathrm{A}} + 4\mathrm{i}\chi|U_0|^2u^{\mathrm{A}} + 9\mathrm{i}\gamma|U_0|^4u^{\mathrm{A}}\\ &\quad - 2\mathrm{i}\chi U_0^2u^{\mathrm{A}*} - 6\mathrm{i}\gamma U_0^3U_0^*u^{\mathrm{A}*} \equiv -\mathcal{P}^{\mathrm{A}}u^{\mathrm{A}}.\end{aligned} \tag{10}$$

It can be checked that the inner product (9) between solutions of equations (7) and (10) is preserved in the evolution. Using this invariance, one can express the inner product, between the quantum perturbation field and a properly chosen projection function, at an output point, $z = L$, in terms of the input quantum perturbation at the initial point $z = 0$.

$$\langle u^{\mathrm{A}}(z=L,t)|\hat{u}(L,t)\rangle = \langle u^{\mathrm{A}}(0,t)|\hat{u}(0,t)\rangle. \tag{11}$$

The relation (11) is the basis of the back-propagation method.

Then, it is easy to calculate the quantum uncertainty of the output field, knowing the statistics of the input quantum-field operators. In particular, the squeezing ratio of an observable,

$$f \equiv \langle f_L(t)|\hat{u}(L,t)\rangle, \tag{12}$$

is calculated as

$$R(L) \equiv \frac{\mathrm{var}[\langle f_L(t)|\hat{u}(L,t)\rangle]}{\mathrm{var}[\langle f_L(t)|\hat{u}(0,t)\rangle]} = \frac{\mathrm{var}[\langle f_0(t)|\hat{u}(0,t)\rangle]}{\mathrm{var}[\langle f_L(t)|\hat{u}(0,t)\rangle]}, \tag{13}$$

where var[·] means the variance, $f_L(t)$ is the projection function at the output point, and $f_0(t)$ is the back-propagated projection function. We will assume that the input quantum perturbation-field operator corresponds to the vacuum state, which is true when the input quantum state is a coherent one. When the noise variation of the perturbed observable of the output state is larger than that of the vacuum state, the squeezing ratio, $R(L)$, is larger than 1. On the other hand, the quantum state gets '*squeezed*' when the noise variation of the perturbed observable in the output state is smaller than that of the vacuum state, $R(L) < 1$. In the case of homodyne detection, the measured perturbed observable is the inner product of the perturbed field operator with the local oscillator pulse [19, 24]. In the usual squeezing experiments for demonstrating the quadrature squeezing, the measurement function $f_L(t)$ is simply described by the following expression (recall that $U_0(z,t)$ is the classical pulse solution in the output),

$$f_L(t) = \frac{U_0(L,t)\mathrm{e}^{\mathrm{i}\theta}}{\sqrt{\int_{-\infty}^{+\infty}\mathrm{d}t\,|U_0(L,t)|^2}}, \tag{14}$$

where θ is an adjustable phase shift between the local oscillator and the signal pulses of the homodyne detection. The optimal (minimum) value of the squeezing ratio $R(z)$ can be chosen by varying the parameter θ. When $\theta = 0$, the in-phase quadrature component is detected, and when $\theta = \pi/2$, the out-of-phase quadrature component is detected. The result of the measurement with another detection phase angle θ can be expressed as a linear combination of the in-phase and out-of-phase quadrature components. Based on the formulation given above, in the next section we will calculate the optimal quadrature squeezing ratios for solitons described by the quantum CQNLSE model.

3. Quadrature squeezing of solitons

3.1. The effects of quintic nonlinearity on quantum fluctuations

To start the analysis of the quantum fluctuations of the CQNLSE solitons, we fix the self-focusing cubic nonlinearity coefficient to be $\chi = +1$ and vary the quintic nonlinearity coefficient γ (see equation (5)), in order to study the effects of quintic nonlinearity on quantum fluctuations. The initial pulse is taken in the form of the CQNLSE soliton, as per equation (3). The optimal squeezing ratio of the soliton quadrature field versus the propagation distance is shown in figure 2. For $\gamma = 0$, the CQNLSE is reduced to the usual cubic NLSE, for which the quantum fluctuations around the soliton have been studied in detail [4]. If $\gamma > 0$, i.e., both the cubic and quintic nonlinearities are focusing, the optimal

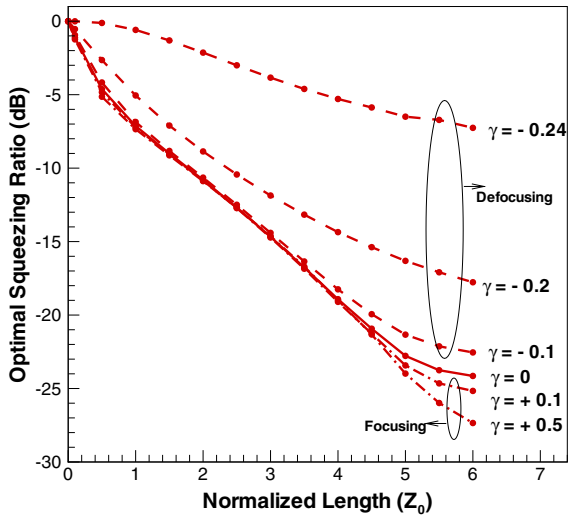

Figure 2. The optimal squeezing ratio as a function of the propagation distance for different values of the strength γ of the quintic nonlinearity, while the cubic-nonlinearity coefficient is fixed, $\chi = 1.0$. When $\gamma > 0$, the squeezing is stronger, while for $\gamma < 0$, it is weaker.

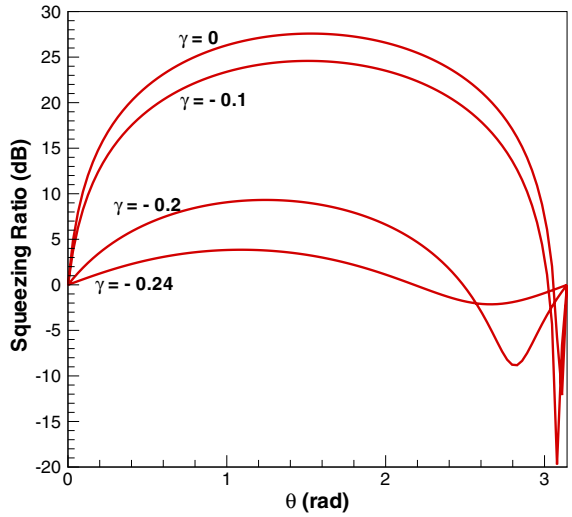

Figure 3. The squeezing ratio as a function of the phase of the local oscillator θ used for homodyne detection. In this case, $\chi = +1.0$, $\gamma < 0$.

quadrature squeezing ratio is almost the same as the case of $\gamma = 0$, if the propagation distance is short, so that the quintic nonlinearity does not essentially affect the CQNLSE soliton. However, for longer distance ($\gtrsim$5 soliton periods), the effect of the quintic nonlinearity accumulates, *improving* the optimal squeezing ratio. On the other hand, the defocusing quintic term with $\gamma < 0$ causes degradation of the optimal squeezing ratio, due to partial compensation between the focusing (cubic) and defocusing (quintic) nonlinearities. If the defocusing quintic term is large ($\gamma = 0.2$), the optimal quadrature squeezing ratio quickly decreases even after propagating a short distance.

Figure 3 shows the dependence of the squeezing ratio on the phase of the local oscillator in the homodyne-detection scheme, in the case when the quintic nonlinearity is defocusing, $\gamma < 0$. This dependence clearly shows the quadrature squeezing of the quantum fluctuations about the CQNLSE

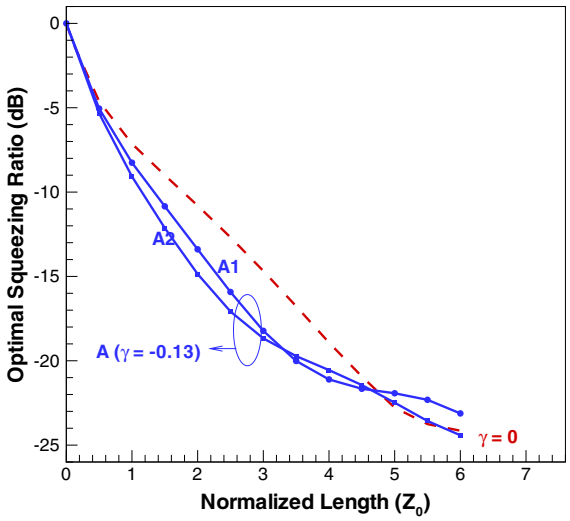

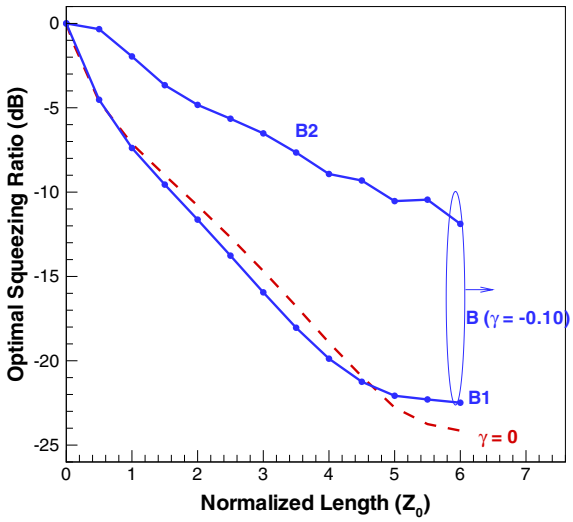

Figure 4. The optimal squeezing ratios for two pairs of bistable solitons. The case of the cubic nonlinear Schrödinger equation, $\gamma = 0$, with the amplitude $A = 1.0$ is also shown (by the dashed curve) for comparison.

solitons, like in the case of the ordinary NLSE solitons ($\gamma = 0$). With the self-focusing quintic term, $\gamma > 0$, the CQNLSE solitons also undergo quadrature squeezing.

3.2. Bistable CQNLSE solitons

Here, we aim to compare the evolution of quantum fluctuations for bistable solitons belonging to the two pairs marked in figure 1. Recall that the pair A is taken at $\gamma = -0.13$, which is close to its turning point, $\gamma = \gamma_{\rm cr}$, and the pair B is taken farther from the respective turning point, at $\gamma = -0.1$. The amplitudes of the solitons are, respectively, $A_1 = 1.3045$, $A_2 = 1.5531$, and $B_1 = 1.147$, $B_2 = 2.033$. The optimal squeezing ratios for these two pairs of bistable solitons are shown in figure 4.

We observe that, for the solitons belonging to the pair A, which have equal widths, $\tau = 3.5$, and slightly different amplitudes, the evolution of the quantum fluctuation is similar. One may expect that the soliton with a higher amplitude will be more squeezed; this is why the optimal squeezing ratio for the

A_2 soliton is smaller than for the A_1 one, in the beginning. But due to the defocusing effect of the quintic nonlinearity (recall that we now consider the case of $\gamma < 0$), the optimal quadrature squeezing ratios for both solitons degrade after propagating a certain distance (about 3 and 4.5 soliton periods for A_2 and A_1, respectively), which leads to the crossing of the squeezing-ratio curves for these bistable solitons.

For the pair B, the difference in the amplitudes in the soliton pair is large. In accordance with this, we find that the properties of the quantum fluctuations are totally different for these two solitons. The curve of the squeezing ratio for the soliton with the smaller amplitude, $B_1 = 1.147$, is like that for the ordinary NLSE solitons (the dashed curve in figure 4), while the squeezing for the soliton with the larger amplitude, $B_2 = 2.033$, is much poorer, which is naturally explained by the strong defocusing effect exerted on the latter soliton by the quintic self-defocusing term.

4. Quantum fluctuations around nonstationary pulses

For situations where exact soliton solutions for pulses are not available, the variational approximation (VA) is known to be an efficient analytical method (for a review see [25]). In particular, the VA for classical CQNLSE solitons was developed in [26], using the Gaussian ansatz for the pulse waveform,

$$U(z,t) = A\exp(-(t^2/2\alpha^2) + \mathrm{i}at^2), \qquad (15)$$

where α and a are, respectively, the width and chirp of the pulse. The use of the Gaussian makes sense not only because it is convenient for the application of VA, but also due to the fact that laser sources usually produce pulses with this shape (including the intrinsic chirp).

Strictly speaking, the Gaussian ansatz may only produce a nonstationary pulse (plus some radiation). Nevertheless, it is still possible to calculate the quantum fluctuation about nonstationary pulses, and compare the results with those presented above for the solitons. Generally, the squeezing ratio for nonstationary pulses cannot be larger than for a soliton of the same width, due to the emission of radiation waves by the nonstationary pulse.

Results of the calculation of the optimal squeezing ratio for Gaussian pulses with different widths are displayed in figure 5. As expected, the Gaussian pulse produces a similar but poorer squeezing curve than the soliton of the same width, $\alpha = 1.25$ (see the dashed–dotted curve, marked by '$\gamma = 0.1$', in figure 5). Better squeezing ratios can be obtained at the short propagation distance for shorter pulses, with $\alpha < 1.25$, but they degrade very quickly with the increase of the distance. For broader pulses, with $\alpha > 1.25$, the radiation modes strongly affect the optimal squeezing ratio from the very beginning.

When $\gamma < 0$, the VA predicts bistable Gaussian pulses for any energy $E_0 = \alpha|A|^2$ [26]. Figure 6 shows the optimal squeezing ratios for a pair of the corresponding bistable nonstationary Gaussian pulses, and they are compared with the curve for the NLSE solitons (marked by '$\gamma = 0$'). This pair of bistable Gaussian pulses have a common width, corresponding to $\alpha = 1.3$ in equation (15), but very different energies, $E_0 = 1.30$ and 6.66. Like in the case of the bistable solitons

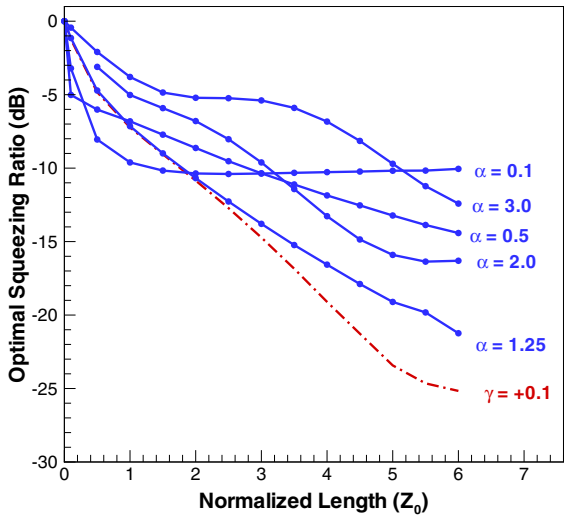

Figure 5. The optimal squeezing ratio versus the propagation distance for different nonstationary Gaussian pulses with different widths. The result for the CQNLSE soliton is plotted by the dashed–dotted curve, for comparison. In this figure, $\gamma = +0.1$, and $A = 1.0$.

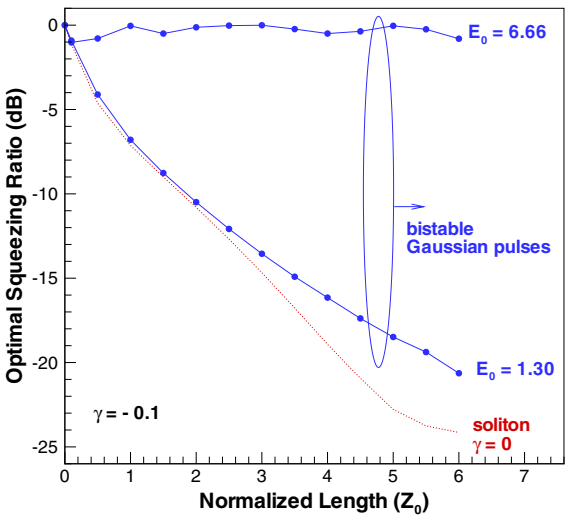

Figure 6. The optimal squeezing ratios for nonstationary bistable Gaussian pulses, in the case of $\gamma = -0.1$ and $\alpha = 1.3$. The squeezing ratio for the ordinary nonlinear-Schrödinger soliton (the dashed–dotted line, $\gamma = 0.0$) is plotted for comparison.

belonging to the pair B in figure 4, the pulse with the smaller energy shows fluctuations similar to those of the NLSE soliton, while the pulse with the larger energy has a much poorer squeezing ratio.

5. Conclusion

In this work, we have applied the back-propagation method to study the quantum fluctuations of bistable solitons described by the cubic–quintic nonlinear Schrödinger equation. It was found that the quadrature-squeezing ratio of the soliton strongly depends on the sign of the quintic nonlinearity: the self-focusing quintic term helps to squeeze the fluctuations, while the self-defocusing one makes the squeezing poorer. In particular, the quantum fluctuations around bistable solitons

with equal widths but different amplitudes seem totally different due to the self-defocusing quintic nonlinearity. Quantum fluctuations of nonstationary Gaussian pulses have also been explored. In that case, emission of radiation by the pulses makes the quadrature squeezing weaker. The result for the nonstationary pulses may provide a useful guideline for the cases in which the exact soliton solutions are hard to find.

The results of this work may be applied to the generation of the nonclassical output from multi-stable solitons in the presence of a higher-order nonlinearity, as well as from multi-dimensional solitons (in the later case, the higher nonlinearity is necessary to prevent collapse). These nonclassical output sources may be useful for processing continuous-variable quantum information.

Acknowledgment

This work was supported in parts by the National Science Council of the Republic of China under Grant No. NSC 93-2752-E-009-009-PAE. BAM appreciates hospitality of the Institute of Electro-Optical Engineering at the National Chiao-Tung University (Hsinchu, Taiwan).

References

[1] Drummond P D and Carter S J 1987 *J. Opt. Soc. Am.* B **4** 1565
[2] Lai Y and Haus H A 1989 *Phys. Rev.* A **40** 844
[3] Lai Y and Haus H A 1989 *Phys. Rev.* A **40** 854
[4] Lai Y and Haus H A 1990 *Phys. Rev.* A **42** 2925
[5] Schmidt E, Knöll L, Welsch D-G, Zielonka M, König F and Sizmann A 2000 *Phys. Rev. Lett.* **85** 3801
[6] Rosenbluh M and Shelby R 1991 *Phys. Rev. Lett.* **66** 153
[7] Bergman K and Haus H A 1991 *Opt. Lett.* **16** 663
[8] Friberg S R, Machida S, Werner M J, Levanon A and Mukai T 1996 *Phys. Rev. Lett.* **77** 3775
[9] Bergé L 1998 *Phys. Rep.* **303** 259
[10] Edmundson D E and Enns R H 1992 *Opt. Lett.* **17** 586
[11] Enns R H and Rangnekar S S 1992 *Phys. Rev.* A **45** 3354
[12] Enns R H, Edmundson D E, Rangnekar S S and Kaplan A E 1992 *Opt. Quantum Electron.* **24** S1295
[13] Kaplan A E 1985 *Phys. Rev. Lett.* **55** 1291
[14] Kaplan A E 1985 *IEEE J. Quantum Electron.* **21** 1538
[15] Herrmann J 1992 *Opt. Commun.* **87** 161
[16] Desyatnikov A, Maimistov A and Malomed B 2000 *Phys. Rev.* E **61** 3107
[17] Mihalache D, Mazilu D, Towers I, Malomed B A and Lederer F 2003 *Phys. Rev.* E **67** 056608
[18] Lai Y and Yu S-S 1995 *Phys. Rev.* A **51** 817
[19] Haus H A and Lai Y 1990 *J. Opt. Soc. Am.* B **7** 386
[20] Smektala F, Quemard C, Couderc V and Barthélémy A 2000 *J. Non-Cryst. Solids* **274** 232
[21] Zhan C, Zhang D, Zhu D, Wang D, Li Y, Li D, Lu Z, Zhao L and Nie Y 2002 *J. Opt. Soc. Am.* B **19** 369
[22] Kolokolov A A 1994 *Izv. Vyssh. Uchebn. Zaved. Radiofiz.* **17** 1332 (in Russian)
[23] Matsko A B and Kozlov V V 2000 *Phys. Rev.* A **62** 033811
[24] Lai Y 1993 *J. Opt. Soc. Am.* B **10** 475
[25] Malomed B A 2002 Variational methods in nonlinear fibre optics and related fields *Progress in Optics* vol 43, ed E Wolf (Amsterdam: Elsevier) p 71
[26] De Angelis C 1994 *IEEE J. Quantum Electron.* **21** 818